Synthesis and characterization of adsorbents for the elimination of nitrates and bromates from water aiming to develop a continuous oxyanion water elimination system

M. Azaro, F. M. Flores, M. Casella, B. Peroni, C. Rodríguez, R. M. Torres Sánchez and M. Jaworski

ABSTRACT

It is known that the excess of oxyanions such as NO_3^- and BrO_3^- in drinking water affects its quality. In this work, three adsorbents (montmorillonite (Mt), silica (Si), and diatomaceous earth) loaded with hexadecyl- (H) and octadecyl-trimethylammonium (O) were used to remove these oxyanions from aqueous solutions by adsorption. In batch systems, the highest NO_3^- removal was obtained with Mt modified with H and O (Mt-H and Mt-O), attaining 33% and 50%, respectively, while for BrO_3^- removal Si modified with H and O, Si-H and Si-O samples, reached 38% and 42%, respectively. A direct relationship between the adsorption capacity of NO_3^- and BrO_3^- and the mass of the adsorbent was found in column filtration tests with Mt-O and Mt-H samples in standard solution and real groundwater samples. The adsorption capacity of the column, in the groundwater sample, remained constant after two reuses.The results obtained are promising for the development of a continuous oxyanion removal system containing the low-cost clay Mt modified with either H or O.

Key words | adsorption, bromate, column filtration, nitrate, organo-montmorillonite

M. Azaro
F. M. Flores (corresponding author)
C. Rodríguez
R. M. Torres Sánchez
CETMIC-CONICET-CCT La Plata-CIC,
Camino centenario y 506, (1897) M. B. Gonnet,
Argentina
E-mail: *mflores@cetmic.unlp.edu.ar*

M. Azaro
M. Casella
B. Peroni
M. Jaworski
CINDECA, CONICET-CCT La Plata, UNLP, CICPBA,
Calle 47 N° 257 (1900) La Plata,
Argentina

M. Jaworski
Facultad de Ingeniería (UNLP),
47 N° 257, La Plata,
Argentina

HIGHLIGHTS

- Three adsorbents were evaluated for oxyanion removal.
- Montmorillonite modified with surfactants was efficient in nitrate removal.
- Silica modified with surfactants was efficient in bromate removal.
- Adsorption column experiments were performed for oxyanion removal.
- The column was successfully reused twice.

INTRODUCTION

Different compounds affect the quality of water intended for human consumption. Among them, there are several oxyanions such as NO_3^-, NO_2^-, BrO_3^-, ClO_3^-, ClO_4^- (Chaplin *et al.* 2012). In particular, NO_3^- is converted to NO_2^- in the human body and can cause oxygen depletion in the blood (Ward *et al.* 2018). In addition, BrO_3^- is generated from Br^- by the ozonation of water to disinfect it and has been classified as a potent carcinogen by the International Agency for Research on Cancer (Moore & Chen 2006).

Adsorption processes play a central role in the development of technologies to eliminate NO_3^- and other water pollutants. Several materials have been used for the adsorption of different anions (Zanella *et al.* 2014; Hu *et al.* 2016; Teimouri *et al.* 2016; Wu *et al.* 2016; Weinertova *et al.* 2017; Singh *et al.* 2018). Clay minerals such as montmorillonite (Mt) have been largely used as adsorbent, due to their high specific surface

doi: 10.2166/ws.2020.324

and low cost. These clays have a laminar structure formed by aluminosilicates that confers negative charges to their surface, being ineffective to remove anions. The presence of hydrated and exchangeable cations in the Mt interlayer, which compensate for its structural negative charges (Torres Sánchez *et al.* 2011), allows tailoring the surface with surfactants, improving its anion adsorption capacity (Santiago *et al.* 2016). Different cationic surfactants have been used to improve the effectiveness of the different adsorbents of inorganic contaminants in waters such as NO_3^- (Thamilarasi *et al.* 2018; Allalou *et al.* 2019). In particular, the modification of Mt with cationic surfactants has been used for water remediation of contaminants with a negative charge (Xi *et al.* 2010; Wang *et al.* 2013).

Amorphous silica or silica gel is produced by the acidification of sodium silicate solutions, generating a gelatinous precipitate that is washed and dehydrated to produce microporous silica. Silica gel is a substance of crystalline appearance, high surface area, and is porous, inert, non-toxic and odorless, chemically stable and insoluble in water or any other solvent. These properties qualify it to act as a selective adsorbent against different molecules (Gammoudi *et al.* 2013).

Diatomaceous earth comes from sedimentary rocks of biogenic origin in whose composition amorphous silica predominates. It consists of skeletons of aquatic organisms called diatoms. This material has a very complex structure, with numerous microscopic pores, cavities, and channels, which gives it a large specific surface, high porosity, and low density. It also has the advantage of being abundant and inexpensive, so its use as a commercial adsorbent has been explored (Sriram *et al.* 2020).

In this sense, this study proposes the modification of an Argentinian Mt, amorphous silica, and diatomaceous earth with two cationic surfactants of different chain length, to evaluate their potential in the remediation of NO_3^- and BrO_3^- ions present in water. The objective is to design a system that allows the adsorption of these anions on different inexpensive materials so that they can be eliminated from groundwater.

MATERIALS AND METHODS

Adsorbents

To obtain the different organo-Mt, montmorillonite (Mt) from North Patagonia, Argentina, was used as received (provided by Castiglioni Pes & Cia.). Its structural formula is $[(Si_{3.89}Al_{0.11})(Al_{1.43}Fe^{3+}_{0.28}Mg_{0.30})O_{10}(OH)_2]Na^+_{0.41}$ (Magnoli *et al.* 2008) and its cation exchange capacity (CEC) = 0.825 mmol g^{-1} (Gamba *et al.* 2015).

An Evonik (before called Degussa) silica (Aerosil 200 with 180 $m^2\ g^{-1}$) was used as a source of SiO_2. This material was treated with an ammonia solution (pH = 10.6) for about 30 min previously to its use (Bideberripe *et al.* 2011).

Commercial diatomaceous earth (Diatomid), consisting of approximately 90% SiO_2 and 10% Al_2O_3, was used without previous treatment.

The surfactants used (see Figure S1 in the Supplementary Material) were octadecyltrimethyl-ammonium bromide (O, provided by Fluka, Buchs, Switzerland), which has a critical micelle concentration CMC = 0.3 mM, purity ≥98% and MW = 392.5 g mol^{-1}, and hexadecyltrimethyl-ammonium bromide (H, purchased from Sigma Aldrich Chemical Company Inc.), which has a CMC = 0.1 mM, purity of 98%, and MW = 364.5 g mol^{-1}. They were used as received.

To obtain the surfactant-modified adsorbents, the corresponding concentrations of O or H surfactant solutions were added to the adsorbents, and the suspension, 10 g L^{-1}, was maintained under stirring (200 rpm) for 2 h at 60 °C. Then, the solids were separated by centrifugation (15,000 rpm) and washed several times with distilled water until no Br^- was detected. Finally, the recovered solid was lyophilized and manually ground in an agate mortar. The prepared adsorbents are listed in Table 1.

Adsorbent characterization

Electrokinetic potentials were determined using Brookhaven 90Plus Bi-MAS. The electrophoretic mobility was converted automatically into zeta potential (Zp) values using the Smoluchowski equation (Miller & Low 1990). The Zp values obtained were used to compare the surface charge of the adsorbents before and after their modification with the respective surfactant. To generate the zeta potential versus pH curves, 40 mg of the samples were dispersed in 40 mL KCl 1 mM solution, used as an inert electrolyte. The slurry was continuously stirred, and the suspension pH was adjusted by adding HCl or KOH.

The surface morphology was characterized by SEM microscopy, using a Philips SEM 50 microscope.

Table 1 | Adsorbents

Adsorbent	Surfactant used	g adsorbent/g surfactant	Sample name	Actual amount of surfactant (% p/p)
Montmorillonite	–	–	Mt	na
	H	0.83	Mt-H	35.0
	O	0.77	Mt-O	58.1
Silica	–	–	Si	na
	H	1	Si-H1	45.4
		1.3	Si-H1.3	36.2
		2	Si-H2	28.4
		4	Si-H4	15.1
		12.5	Si-H12.5	3.0
	O	1	Si-O1	nd
		1.25	Si-O1.25	nd
Diatomaceous earth	–	–	D	na
	H	1	D-H1	nd
		2	D-H2	nd
	O	1	D-O1	nd
		2	D-O2	nd

na, not applicable.
nd, not determined.

The actual surfactant loading of the adsorbents that presented the best adsorption capacity was determined by thermogravimetric analysis (TG/TGA, NETZSCH STA 409 PC/PG) with alumina as reference. The adsorbents, 20 mg, were placed in alumina crucibles and heated from 30 °C to 800 °C at a scan rate of 10 °C min^{-1} in the air atmosphere. The actual surfactant loading for the samples was determined from the mass loss values in the temperature range from 150° C to 800 °C, taking into account the mass loss of Mt structural hydroxyl groups (Xie *et al.* 2001).

Batch adsorption studies

Adsorption experiments were performed by placing 0.1 g of the respective samples in a 100 mL glass bottle containing 50 mL of a solution of 100 mg L^{-1} of NO_3^- or 50 mg L^{-1} of BrO_3^-. Suspensions were maintained under continuous mechanical stirring for 24 h. The experiments were performed in duplicate. The pH of the suspensions was allowed to evolve naturally.

After the contact time, the suspensions were centrifuged at 15,000 rpm for 15 min to recover the solids. The supernatant was analyzed by ion chromatography (IC, Metrohm 790 Personal IC) to determine NO_3^- and BrO_3^- concentration. As a mobile phase, $NaHCO_3$ 1.0 mM and Na_2CO_3 3.2 mM solutions were used at a flow rate of 7 mL min^{-1}.

The amount of adsorbed NO_3^-, Q_{ADS}, (mg NO_3^- g^{-1} clay) was determined according to:

$$Q_{ADS} = \frac{(C_i - C_e) \cdot V}{m}$$

where C_i and C_e are the initial and equilibrium anion concentration, respectively, V is the anion solution volume (mL) and m is the adsorbent mass (mg).

The adsorbent that attained the highest NO_3^- and BrO_3^- adsorption in aqueous solutions was also evaluated in water samples taken from the Puelche Aquifer, and the NO_3^- concentration of these water samples was measured before the adsorption test (Wu *et al.* 2016). The Puelche Aquifer is one of the water reservoirs in Argentina that supplies drinking water to the most densely populated areas in Argentina such as the Buenos Aires Metropolitan Region. This aquifer has low salinity, approximately 585 mg L^{-1}, and its drinkability is only affected by the NO_3^- content, especially in urbanized areas (Zabala *et al.* 2016; Armengol *et al.* 2017).

Effect of pH

The effect of pH on NO_3^- removal by Mt-H was evaluated by using 0.1 g Mt-H and 50 mL NO_3^- solution 100 mg L^{-1} (pH 7.7) added into the flasks. The pH of the solution was adjusted to 3.2 and 5.0 using HCl 0.1 M. The flasks were shaken for 24 h, and the solutions recovered after the centrifugation process of these samples were analyzed by IC.

Adsorption isotherms

To perform the adsorption isotherms, NO_3^- solutions were prepared by diluting a 1,000 mg L^{-1} stock solution in deionized water. The adsorption of NO_3^- was conducted using the best adsorbent determined in the batch adsorption studies (Mt-H sample). Then, 0.1 g of adsorbent and 50 mL NO_3^- solution (25, 50, 75, 100, 150, and 200 mg L^{-1}) were placed in 100 mL glass bottles. The pH of the suspensions was allowed to evolve naturally during the experiments.and the glass bottles were maintained under stirring for 24 h at 25 °C. After this contact time, the supernatant was removed by centrifugation and analyzed by IC.

Isotherms were fitted using different mathematical models widely applied in the liquid/solid adsorption processes, Langmuir, Freundlich, and Sips models.

The Langmuir model assumes monolayer adsorption on finite, identical, and equivalent sites. However, it does not predict lateral interactions or steric hindrance, even between adjacent adsorbate molecules (Foo & Hameed 2010). The mathematical expression of the Langmuir isotherm model is:

$$Q_{ADS} = \frac{Q_{max.K_L}.C_e}{1 + K_L \cdot C_e}$$

where Q_{ADS} (mg g^{-1}) is the NO_3^- adsorbed amount, Q_{max} (mg g^{-1}) is the theoretical maximum adsorption capacity, K_L (L mg^{-1}) is the Langmuir constant (or affinity constant), and C_e (mg L^{-1}) is the equilibrium concentration. Normally, for good adsorbents a high K_L and high Q_{max} are suitable (Marco-Brown *et al.* 2014).

The Freundlich model does not predict monolayer adsorption and can be applied to multilayer adsorption. This model describes non-ideal and reversible adsorption on a heterogeneous surface (Foo & Hameed 2010). The expression of the Freundlich equation is the following:

$$Q_{ADS} = (K_F \cdot C_e)^{1/n}$$

where K_F (L $g^{-1})^{1/n}$ is the Freundlich constant related to the adsorbed capacity, and $1/n$ is a dimensionless number that characterizes the system heterogeneity (Sandy *et al.* 2012; Aljerf 2018).

The Sips model is a Langmuir and Freundlich model combination. At low adsorbate concentration, its behavior is similar to that of the Freundlich model and at higher adsorbate concentrations it predicts monolayer adsorption like the Langmuir isotherm (Foo & Hameed 2010). The mathematical form of the Sips model is:

$$Q_{ADS} = \frac{Q_{max.}(K_S \cdot C_e)^{1/n}}{1 + (K_S \cdot C_e)^{1/n}}$$

where K_S (L mg^{-1}) is the Sips constant or affinity coefficient (Sandy *et al.* 2012).

Column filtration studies

The columns of different lengths were filled with a mixture of commercial quartz sand (Cicarelli, particle size 0.106–0.850 mm) and 2 wt% of the adsorbents. To prevent the filling loss, glass wool was placed in the lower and upper parts of the column. Then, the sand and adsorbent mixture, previously mixed manually, was slowly added to the column (filling length: 2.5, 3.0, and 3.5 cm).

The column was conditioned with the passage of a slow flow of deionized water from the bottom to top, to prevent the formation of preferential paths during elution. After the column was conditioned, a constant rate flow at 2.6 mL min^{-1} of a solution containing 100 mg L^{-1} of NO_3^- or 50 mg L^{-1} of BrO_3^- was passed through the column, and aliquots were taken at different filtered volumes to evaluate the removal of the respective anions. Figure S2 (Supplementary Material) shows the column diagram of the system used to remove the anions. In the diagram, there is a reservoir that contains the solution of NO_3^- or BrO_3^- that is passed through the column using a peristaltic pump.

Desorption experiments

Desorption experiments were carried out immediately after the adsorption by passing a solution of 1 M NaCl through the column at a flow rate of 2.5 mL min^{-1}. This column was reused with a new solution of NO_3^- 100 mg L^{-1}. The effluent was collected at regular intervals, and this procedure was repeated twice.

RESULTS AND DISCUSSION

Adsorbent characterization

The morphology of some absorbents was analyzed by SEM before and after the adsorption process, to observe changes in these materials.

The SEM images of diatomaceous earth (Figue S3, Supplementary Material) showed the presence of fossil microorganisms. No significant modifications in the structure were observed in the diatomaceous earth (Figure S3b) after its modification with the surfactant O or after being used in the batch adsorption system (Figure S3c).

Figure 1 shows the curves of Zp values as a function of the pH of unmodified and modified adsorbents with ODTMA. It can be seen that Zp values are negative for the unmodified adsorbents and become positive when the adsorbents are modified with O. In our previous work, it was demonstrated that the sign of the Zp is significantly modified by the different chain lengths of the surfactant (Jaworski *et al.* 2019). For the same adsorbents modified with *H*, a similar tendency was observed (Figure S4, Supplementary Material).

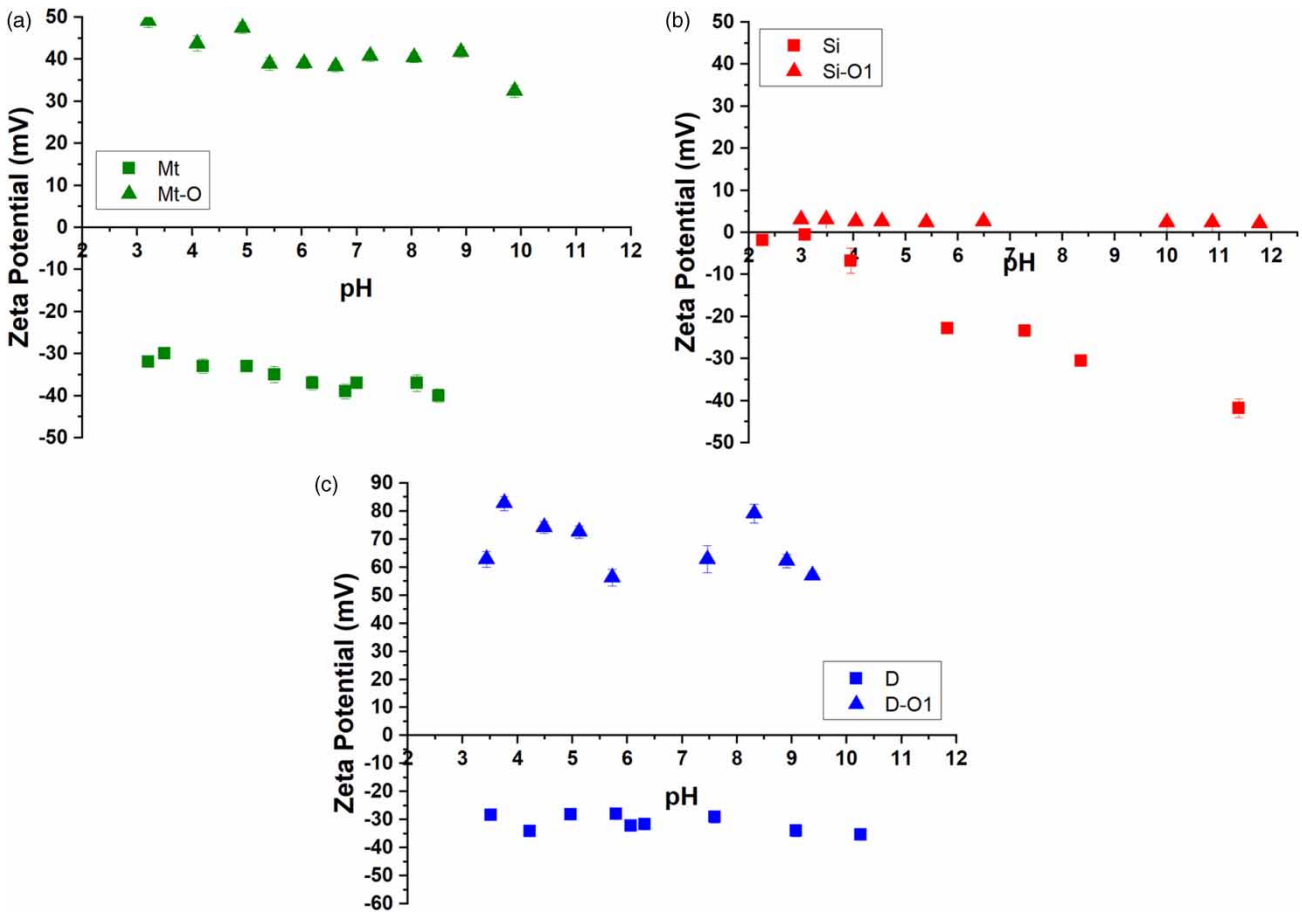

Figure 1 | Zeta potential of adsorbents: (a) Mt, (b) Si and (c) diatomaceous earth (D).

Batch adsorption studies

Figure 2(a) and 2(b) show the removal (%R) of NO_3^- and BrO_3^- respectively. The results obtained showed a great increase in NO_3^- and BrO_3^- removal using the surfactant-modified adsorbents, which is almost zero in the unmodified adsorbents. This behavior could be related to the surface charge sign of each adsorbent, which is positive for those modified with surfactants (anion attraction) and negative for the unmodified ones (anion repulsion).

In the results obtained from Figure 2, it is important to note that there is a relation between the amount of surfactant loaded (see Table 1) and anion removal. In addition, higher NO_3^- removal was obtained with the surfactant with the largest chain length (O) in agreement with the results found in previous work (Jaworski *et al.* 2019).

The highest NO_3^- removal was achieved using the Mt modified with both surfactants (Mt-H and Mt-O), while the highest BrO_3^- removal was obtained with silica samples (Si-H1, Si-H1.3 and Si-O1).

Effect of pH

The effect of the pH on NO_3^- removal in a batch system using the adsorbent Mt-H was studied (Figure 3). The NO_3^- removal was performed at three different pH values: 3.2, 5.0, and 7.7. As shown in Figure 3, there are no significant changes in NO_3^- removal with the different pH values evaluated. This could be because the surface charge remains practically constant in all pH ranges (Figure 1).

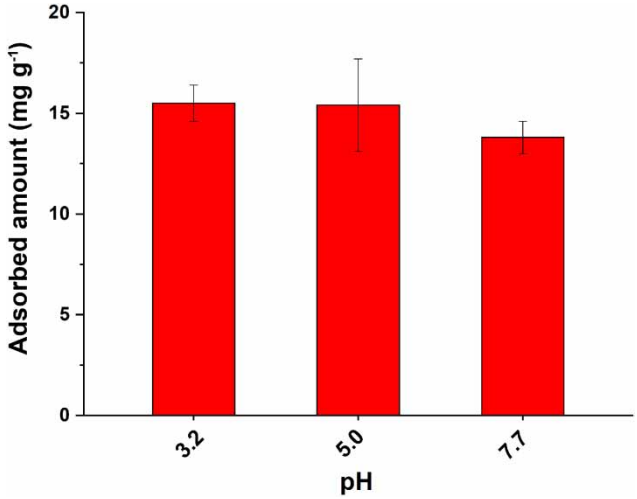

Figure 3 | Effects of pH on NO_3^- adsorption on the Mt-H sample at room temperature.

Adsorption isotherms

The adsorption isotherm of NO_3^- on the Mt-H sample is shown in Figure 4. The amount of NO_3^- adsorbed increases rapidly at low initial concentrations. As the concentration increases, the saturation of the system is reached, and the adsorption remains constant. The Langmuir, Freundlich, and Sips isotherm

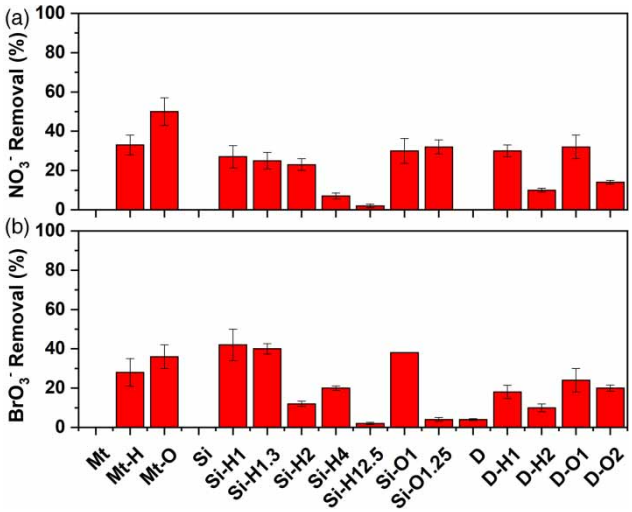

Figure 2 | % Removal of (a) NO_3^- and (b) BrO_3^- by indicated adsorbents.

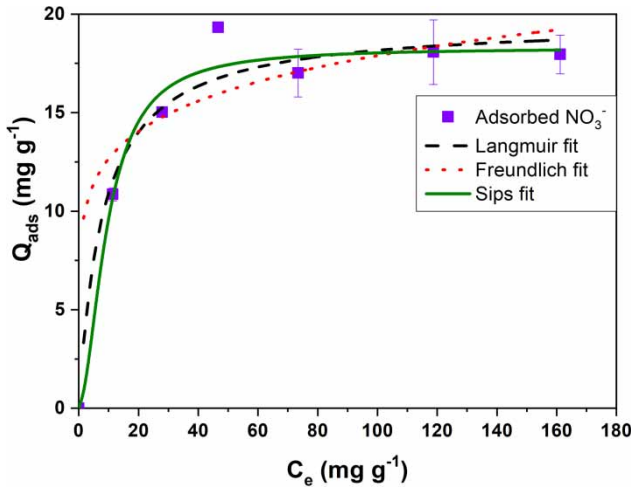

Figure 4 | NO_3^- adsorption isotherms on Mt-H sample.

models were applied to determine the related parameters for NO_3^- adsorption on the Mt-H sample in aqueous media.

The Langmuir, Freundlich, and Sips parameters obtained are summarized in Table 2. The best fit to the experimental adsorption points was obtained by the Sips model. This model predicts that the adsorption system, at low concentrations of NO_3^-, would behave in a heterogeneous form, as predicted also by the Freundlich model. However, at high NO_3^- concentrations, the adsorption would occur in a homogeneous form, and as a monolayer.

The Q_{max} obtained with Sips fit was 18 mg g^{-1}, similar to the experimental value found, and the $1/n$ value was close to 1, which could indicate low surface heterogeneity.

Column adsorption studies

As was described previously, the synthesized adsorbents were evaluated in a batch system (Figure 2) using NO_3^- and BrO_3^- solutions prepared in deionized water. However, the use of batch systems to remove oxyanions from a large volume of water would be expensive. As a technological application, the column filtration systems are considered a better economic alternative. Column filtration systems using organo-Mt and sand mixtures have been previously reported to yield good results in perchlorate and thiophanate-methyl removal (Nir *et al.* 2015; Flores *et al.* 2020).

The first experiments were done with the column of length 2.5 cm, and the adsorbents in a proportion of 2 wt% concerning filling weight. The adsorbents used were D-H1, Si-H1, Mt-H, and Mt-O. With the column containing D-H1, the adsorbent eluted along the column with the NO_3^- solution, and with the column containing Si-H1, the surfactant was released from the silica and eluted through the column. Therefore, the results obtained with the adsorbents based on diatomaceous earth and silica are not shown in the column filtration studies. The column study using the Mt without surfactant is not included either. Due to the high water retention of this clay, the column swells, and it is difficult to take water samples.

The column filtration results of NO_3^- and BrO_3^- performed with Mt-H and Mt-O samples are presented in Figure 5. The NO_3^- and BrO_3^- removal in the columns filled with Mt-O and Mt-H samples (Figure 5) decreases with the filtered volume, being lower for the Mt-H than for the Mt-O sample, in agreement with the results obtained for batch systems (Figure 2). The column filled with the Mt-H sample, after 30 mL filtered volume of NO_3^- solution, attained approximately 10% removal, reaching almost the saturation of the column (Figure 5(a)). For the Mt-O column, after 40 mL filtered volume, NO_3^- removal remained at 30%.

The BrO_3^- removal (Figure 5(b)) presented a faster saturation than that obtained for NO_3^- for both adsorbents (Mt-O and Mt-H samples). For that reason, the influence of the filling height and desorption experiments were carried out using NO_3^- solution sand, due to the lower toxicity of H than O (Orta *et al.* 2019) with the Mt-H adsorbent.

Table 2 | Langmuir, Freundlich and Sips parameters for NO_3^- adsorption on Mt-H sample

Langmuir model			
Q_{max} (mg g^{-1})	K_L (L mg^{-1})		R^2
20 ± 1	0.12 ± 0.04		0.7789
Freundlich model			
K_F (L $g^{-1})^{1/n}$	$1/n$		R^2
9 ± 2	0.15 ± 0.06		0.5365
Sips model			
Q_{max} (mg g^{-1})	K_S (L mg^{-1})	$1/n$	R^2
18 ± 1	0.11 ± 0.02	1.8 ± 0.8	0.96831

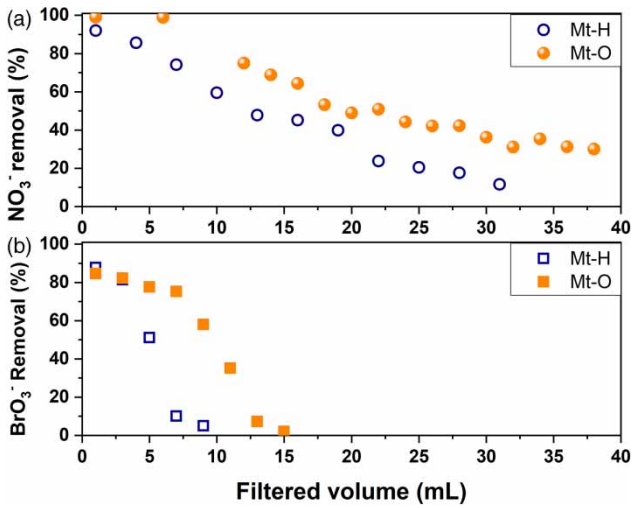

Figure 5 | The percentage removal of (a) NO_3^- and (b) BrO_3^- using columns with a filling height of 2.5 cm.

Influence of the filling height

In order to evaluate the influence of the operational conditions on NO_3^- removal, the column filtration experiments were carried out at different filling heights (Figure 6). The adsorption capacity increased with the filling length for the column that reached saturation (15.47 mg g^{-1} and 19.15 mg g^{-1}, for 2.5 cm and 3.0 cm, respectively). For the column with the highest filling height (3.5 cm), the saturation capacity was not reached in the filtered volume analyzed (Figure 6) and for this reason, NO_3^- adsorption capacity was lower than that obtained for the shorter columns (11.71 mg g^{-1}). The general trend is an increase in the adsorption capacity of NO_3^- with the increase in filling length, indicating that the longer contact time between NO_3^- and the adsorbent, generated by the length of the column filling, produced the increase of the adsorption capacity (Wu *et al.* 2016).

Desorption and reuse assay

To test the reusability of the Mt-H column, NaCl 1M was used as eluent. The NO_3^- was removed and then, the column was reused with a fresh NO_3^- solution. These adsorption–desorption cycles were repeated twice (Figure 7). The obtained adsorption capacity values were 19.15 mg g^{-1} and up to 21.74 mg g^{-1} for initial adsorption, cycle 1 and 2, respectively.

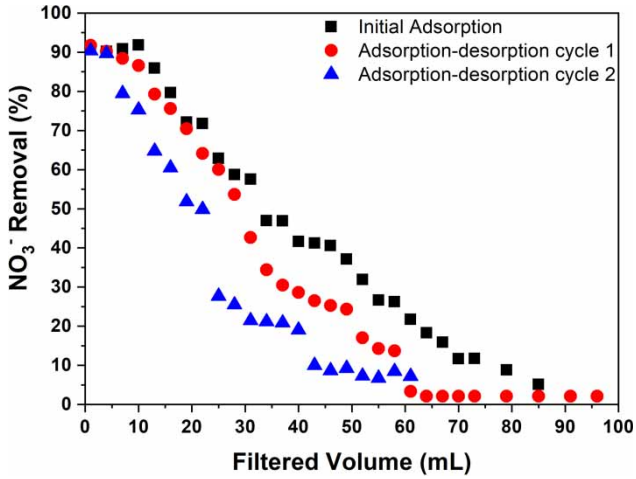

Figure 7 | Adsorption–desorption cycles for NO_3^- removal with Mt-H columns.

In the first cycle, NO_3^- desorption was 72% after the passage of 37 mL of NaCl. This column was reused with a fresh NO_3^- solution, and the adsorption capacity increased up to 13.5%. In the second desorption cycle, its value was 51% after passing the same volume of 1 M NaCl as in the first cycle. However, by reusing the column, the adsorption capacity remained constant.

In order to further investigate the applicability of the Mt-H columns in environmental conditions, the column (filling height: 2.5 cm) was used with groundwater extracted from one of the largest aquifers in Argentina (Figure 8). The groundwater characteristics were: NO_3^- initial concentration of 60 mg L^{-1} and the presence of mostly bicarbonate.

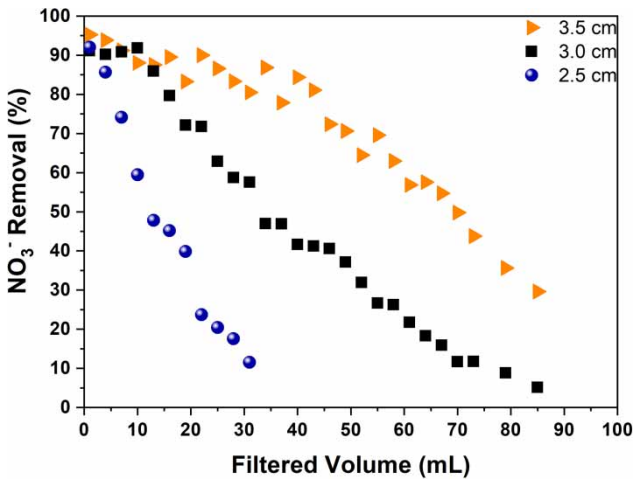

Figure 6 | Effect of different filling heights for column filtration experiments, using NO_3^- solution and Mt-H sample.

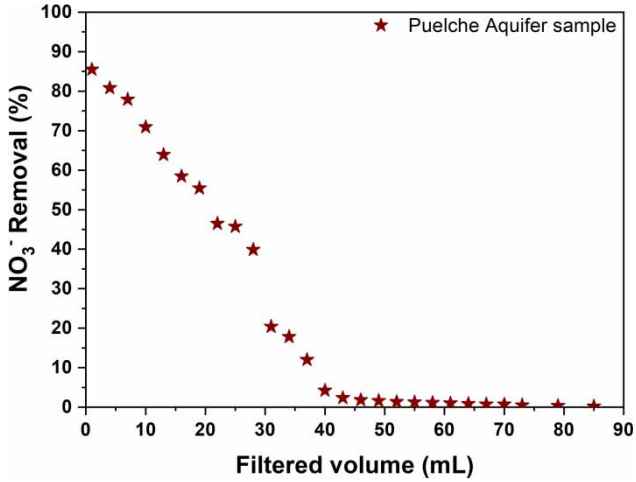

Figure 8 | Removal of NO_3^- (%) using groundwater as a function of the filtered volume with a column containing Mt-H.

The saturation of the column was reached after 40 mL of elution, similar to that observed for standard NO_3^- solution (Figure 6). However, since the initial NO_3^- concentration for groundwater was less than that of the standard solution, it cannot be ruled out that the presence of other anions may be competing with NO_3^-. The NO_3^- adsorption capacity was 10.67 mg g^{-1}, around 69% of the capacity observed for a standard solution.

The results obtained for columns filled with the low-cost and available Mt modified with H are promising for technological use.

CONCLUSIONS

In this work, three different adsorbents (montmorillonite, silica, and diatomaceous earth) unmodified and modified with cationic surfactants (H and O) were used to adsorb NO_3^- and BrO_3^- ions in a batch and column system. The higher adsorption attained by the modified adsorbents than by the respective unmodified ones was associated with the generation of positive surface electric charge with the surfactant loading, evidenced by the zeta potential values, which increased the surface interaction with the anions. Within the adsorbents assayed, organo-Mt adsorbed mostly NO_3^-, while the SiO_2-based adsorbents removed the largest amount of BrO_3^-. In the column filtration studies using Mt-H and Mt-O, progressive removal of NO_3^- was observed based on the filtered volume, which indicates a promising technological application for removal of these water anions. Concerning NO_3^- removal from real groundwater, we observe that the presence of other anions such as bicarbonate probably interferes with NO_3^- adsorption.

CONFLICTS OF INTEREST

The authors declare that there are not conflicts of interest.

ACKNOWLEDGEMENTS

This work has been funded by the following projects: PICT 1391 and 1178, Project UNLP X700, and X802. M.A. and F.M.F. thank CIC-PBA and CONICET, respectively, for the grant received.

DATA AVAILABILITY STATEMENT

All relevant data are included in the paper or its Supplementary Information.

REFERENCES

Aljerf, L. 2018 High-efficiency extraction of bromocresol purple dye and heavy metals as chromium from industrial effluent by adsorption onto a modified surface of zeolite: kinetics and equilibrium study. *Journal of Environmental Management* **225**, 120–132.

Allalou, O., Miroud, D., Belmedani, M. & Sadaoui, Z. 2019 Performance of surfactant-modified activated carbon prepared from dates wastes for nitrate removal from aqueous solutions. *Environmental Progress & Sustainable Energy* **38** (S1), S403–S411.

Armengol, S., Manzano, M., Bea, S. A. & Martínez, S. 2017 Identifying and quantifying geochemical and mixing processes in the Matanza-Riachuelo Aquifer System, Argentina. *Science of The Total Environment* **599–600**, 1417–1432.

Bideberripe, H. P., Ramallo-López, J. M., Figueroa, S. J. A., Jaworski, M. A., Casella, M. L. & Siri, G. J. 2011 Ge-modified Pt/SiO_2 catalysts used in preferential CO oxidation (CO-PROX). *Catalysis Communication* **12** (14), 1280–1285.

Chaplin, B. P., Reinhard, M., Scheneider, W. F., Schüth, C., Sharpley, J. R., Strathmann, T. J. & Werth, C. J. 2012 Critical review of Pd-based catalytic treatment of priority contaminants in water. *Environmental Science & Technology* **46**, 3655–3670.

Flores, F. M., Undabeytia, T., Jaworski, M., Morillo, E. & Torres Sánchez, R. M. 2020 Organo-montmorillonites as adsorbed materials for thiophanate-methyl removal: adsorption–desorption studies and technological applications. *Journal of Environmental Chemical Engineering* **8**, 103806.

Foo, K. Y. & Hameed, B. H. 2010 Insights into the modeling of adsorption isotherm systems. *Chemical Engineering Journal* **156** (1), 2–10.

Gamba, M., Flores, F. M., Madejová, J. & Torres Sánchez, R. M. 2015 Comparison of Imazalil removal onto montmorillonite and nanomontmorillonite and adsorption surface sites involved: an approach for agricultural wastewater treatment. *Industrial & Engineering Chemistry Research* **54**, 1529–1538.

Gammoudi, S., Frini-Srasra, N. & Srasra, E. 2013 Preparation, characterization of organosmectites and fluoride ion removal. *International Journal of Mineral Processing* **125**, 10–17.

Hu, Q., Chen, N., Feng, C., Zhang, J., Hu, W. & Lv, L. 2016 Kinetic studies of nitrate removal from aqueous solution using granular chitosan-Fe(III) complex. *Water Science & Technology* **73** (5), 1211–1220.

Jaworski, M. A., Flores, F. M., Fernández, M. A., Casella, M. & Torres Sánchez, R. M. 2019 Use of organo-montmorillonite for the nitrate retention in water: infuence of alkyl length of loaded surfactants. *SN Applied Sciences* **1**, 1318.

Magnoli, A. P., Tallone, L., Rosa, C. A. R., Dalcero, A. M., Chiacchiera, S. M. & Torres Sanchez, R. M. 2008 Commercial bentonites as detoxifier of broiler feed contaminated with aflatoxin. *Applied Clay Science* **40** (1–4), 63–71.

Marco-Brown, J. L., Areco, M. M., Torres Sánchez, R. M. & dos Santos Alfonso, M. 2014 Adsorption of picloram herbicide on montmorillonite: kinetic and equilibrium studies. *Colloids and Surfaces A: Physicochemical and Engineering Aspects* **449**, 121–128.

Miller, S. E. & Low, P. F. 1990 Characterization of the electrical double layer of montmorillonite. *Langmuir* **6** (3), 572–578.

Moore, M. M. & Chen, T. 2006 Mutagenicity of bromate: implications for cancer risk assessment. *Toxicology* **221** (2–3), 190–196.

Nir, S., Brook, I., Anavi, Y., Ryskin, M., Ben-Ari, J., Shveky-Huterer, R., Etkin, H., Zadaka-Amir, D. & Shuali, U. 2015 Water purification from perchlorate by a micelle–clay complex: laboratory and pilot experiments. *Applied Clay Science* **114**, 151–156.

Orta, M. M., Flores, F. M., Fernández Morantes, C., Curutchet, G. & Torres Sánchez, R. M. 2019 Interrelations of structure, electric surface charge, and hydrophobicity of organo-mica and montmorillonite, tailored with quaternary or primary amine cations. Preliminary study of pyrimethanil adsorption. *Materials Chemistry and Physics* **223**, 325–335.

Sandy, Maramis, V., Kurniawan, A., Ayucitra, A., Sunarso, J. & Ismadji, S. 2012 Removal of copper ions from aqueous solution by adsorption using laboratories modified bentonite (organo-bentonite). *Frontiers of Chemical Science and Engineering* **6**, 58–66.

Santiago, C. C., Fernández, M. A. & Torres Sánchez, R. M. 2016 Adsorption and characterization of MCPA on DDTMA- and raw-montmorillonite: surface sites involved. *Journal of Environmental Science and Health, Part B* **51** (4), 245–253.

Singh, N. B., Nagpal, G., Agrawal, S. & Rachna, 2018 Water purification by using adsorbents: a review. *Environmental Technology & Innovation* **11**, 187–240.

Sriram, G., Uthappa, U. T., Rego, R. M., Kigga, M., Kumeria, T., Jung, H. Y. & Kurkuri, M. D. 2020 Ceria decorated porous diatom-xerogel as an effective adsorbent for the efficient removal of Eriochrome Black T. *Chemosphere* **238**, 124692.

Teimouri, A., Nasab, S. G., Vahdatpoor, N., Habibollahi, S., Salavati, H. & Chermahini, A. N. 2016 Chitosan/Zeolite Y/nano ZrO_2 nanocomposite as an adsorbent for the removal of nitrate from the aqueous solution. *International Journal of Biological Macromolecules* **93** (Part A), 254–266.

Thamilarasi, M. J. V., Anilkumar, P., Theivarasu, C. & Sureshkumar, M. V. 2018 Removal of vanadium from wastewater using surface-modified lignocellulosic material. *Environmental Science and Pollution Research* **25**, 26182–26191.

Torres Sánchez, R. M., Genet, M. J., Gaigneaux, E. M., dos Santos Afonso, M. & Yunes, S. 2011 Benzimidazole adsorption on the external and interlayer surfaces of raw and treated montmorillonite. *Applied Clay Science* **53** (3), 366–373.

Wang, W., Zhou, J., Wei, D., Wan, H., Zheng, S., Xu, Z. & Zhu, D. 2013 ZrO_2-functionalized magnetic mesoporous SiO_2 as effective phosphate adsorbent. *Journal of Colloid and Interface Science* **407**, 442–449.

Ward, M. H., Jones, R. R., Brender, J. D., de Kok, T. M., Weyer, P. J., Nolan, B. T., Villanueva, C. M. & van Breda, S. G. 2018 Drinking water nitrate and human health: an updated review. *International Journal of Environmental Research and Public Health* **15** (7), 1557.

Weinertova, K., Honorato, R. S., Stranska, E. & Nedela, D. 2017 Comparison of heterogeneous anion-exchange membranes for nitrate ion removal from mixed salt solution. *Chemical Papers* **72**, 469–478.

Wu, Y., Wang, Y., Wang, J., Xu, S., Yu, L., Corvini, P. & Wintgens, T. 2016 Nitrate removal from water by new polymeric adsorbent modified with amino and quaternary ammonium groups: batch and column adsorption study. *Journal of the Taiwan Institute of Chemical Engineers* **66**, 191–199.

Xi, Y., Mallavarapu, M. & Naidu, R. 2010 Preparation, characterization of surfactants modified clay minerals and nitrate adsorption. *Applied Clay Science* **48** (1–2), 92–96.

Xie, W., Gao, Z., Liu, K., Pan, W., Vaia, R., Hunter, D. & Singh, A. 2001 Thermal characterization of organically modified montmorillonite. *Thermochimica Acta* **367–368**, 339–350.

Zabala, M. E., Martínez, S., Manzano, M. & Vives, L. 2016 Groundwater chemical baseline values to assess the recovery plan in the Matanza-Riachuelo River basin, Argentina. *Science of The Total Environment* **541**, 1516–1530.

Zanella, O., Tessaro, I. C. & Féris, L. A. 2014 Study of $CaCl_2$ as an agent that modifies the surface of activated carbon used in sorption/treatment cycles for nitrate removal. *Brazilian Journal of Chemical Engineering* **31** (1), 205–210.

First received 8 July 2020; accepted in revised form 3 November 2020. Available online 17 November 2020